

SEDIMENTATION AND SEDIMENT FLUSHING PROCESSES IN RESERVOIRS

広島大学大学院 学生会員 ○Julio Masis 広島大学工学部 フェロー会員 福岡捷二
広島大学工学部 正会員 渡邊明英 姫路市役所 正会員 鶴尾和樹

1. Introduction:

In order to implement a sediment removal technique in a reservoir, it is necessary to foresee the process of deposition and the response to the application of a technique like the sediment flushing by water surface drawdown. In this investigation the processes of front formation and sediment flushing were investigated by means of laboratory experiments and numerical computations assuming one-dimensional character.

2. Experimental method:

A dam facility with a bottom gate was installed at the downstream end of a re-circulating straight flume. Figure 1 shows the system. Water surface elevations were measured continuously at seven locations. Longitudinal bed profiles were measured at different times along the flume-center line every 10 cm. The bed material used was silica sand with uniform size distribution, D_{50} equal to 0.0008 m and the specific gravity to 2.65.

The channel plan-shape is shown in Figure 2. It has three sections with different widths, to stimulate sediment transport in the upstream reaches and deposition near the dam.

To perform the front formation runs, the bed was initially flat, the influent discharge was constant and the water surface elevation controlled by the dam height. No sediment supply was done therefore, degradation occurred in the upper reaches as the bed began to stabilize.

To perform the sediment flushing runs, the bottom gate was opened manually to allow for water surface drawdown near the dam producing higher velocities and scoring the deposits. Finally the eroded material was expelled through the bottom gate at the dam. Different initial bed conditions were employed, for flushing run F0 an initial flat bed with low bottom gate elevation was employed, in the others, instead, the bed configuration obtained in previous front-formation runs was employed together with different bottom gate elevations. Thus, it was possible to observe the front erosion as the water drawdown progressed.

Bed transients were measured after closing the gate. Later, the flushing process was restarted. The sediment discharge was collected manually in alternate intervals of 30 seconds in one case. Table 1 summarizes the conditions for each experiment. For deposition runs two different discharges were used.

In this paper only few examples of deposition and flushing runs are shown to illustrate such processes.

3. Numerical method:

The developed model solves the Saint Venant's equations including the longitudinal change of width.

For momentum and water continuity:

$$\frac{\partial Q}{\partial t} + \frac{\partial(Qv + gAh)}{\partial x} + gA(S_f - S_0) - \frac{gh^2}{2} \frac{\partial B(x)}{\partial x} = 0$$
$$\frac{\partial A}{\partial t} + \frac{\partial Q}{\partial x} = 0 \quad S_0 = \frac{\partial Z_b}{\partial x} \quad S_f = \frac{n^2 v^2}{R_h^{4/3}}$$

For sediment continuity:

$$(1 - \lambda) \frac{\partial(z_b)}{\partial t} + \frac{1}{B(x)} \frac{\partial Q_s}{\partial x} = 0 \quad Q_s = B(x)q_s$$

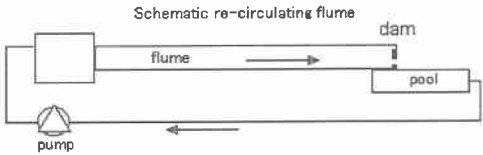


Figure 1. Sketch of the flume for experiments.

Scheme of the narrow flume for the sediment deposition and hydraulic Flushing

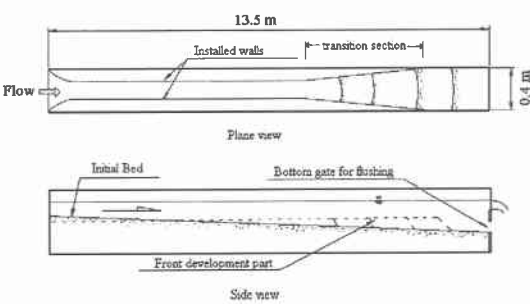


Figure 2. Schematic sketch for front formation

Table 1: Conditions for the experiments

Run D=Deposition F=Flushing	Initial Bed Slope	Gate Elevation (m)	Influent Discharge (m3/s)
D1	0.0064	0.22*	0.0055
D2		0.22*	0.0082
F0	0.0031	0.11	0.0061
F1	-----	0.19	0.0055
F2		0.19	0.0065
F3		0.19	0.0048
F4		0.22	0.0064

* Bed elevation at the dam

Sediment transport equations:

Ashida - Michiue formula :

$$\frac{q_s}{\sqrt{sgd^3}} = 17\tau_*^{3/2} \left[1 - \frac{\tau_* c}{\tau_*} \right] \left[1 - \frac{u_* c}{u_*} \right]$$

Meyer - Peter & Muller formula

$$\frac{q_s}{\sqrt{sgd^3}} = 8[\tau_* - 0.047]^{3/2}$$

The sediment transport was estimated using Ashida-Michiue and Meyer-Peter&Muller equations. The method of finite differences using the explicit predictor-corrector **MacCormack scheme** was implemented in the discretization.

The simultaneous change of bed with the water transients at every computational time step was included, so the model can be considered as coupled. The appropriate boundary conditions were provided for both types of runs.

From the calibration of the hydrodynamic component, the Manning's resistance coefficient was fixed to 0.0135. Also, a correction of the sediment transport equations was necessary to account for the additional resistance produced by the wavy bed and the effect of the walls (values of width/depth<6).

4. Comparison of the experimental and numerical results:

- **Sediment deposition runs:** The front was observed to grow in size and moved toward the dam. It started developing just few centimeters downstream from the point where the walls started to diverge. The bed aggraded rapidly producing a sudden increase in bed elevation until a limiting or critical depth was reached, after that, the front developed almost horizontally. Figure 3 shows the front formation process at different times as observed and as computed by the numerical model. Figure 4 shows observed and computed results of the

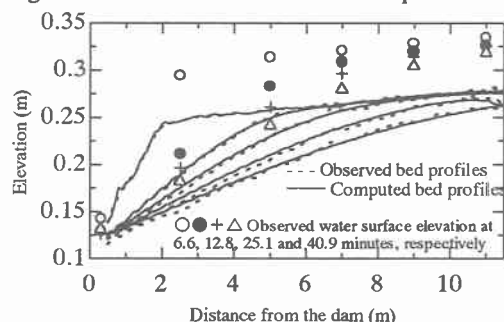


Figure 5: Experimental and calculated results for run F0

position and displacement velocity of the front in time. The front velocity decreased as the channel width increased, becoming nearly constant after 0.55 hours corresponding to the time at which the front reached the widest region. In both graphs, the agreement between the computed and observed results is good.

- **Sediment flushing runs:** Figure 5 shows the observed bed and water surface transients at different times for run F0 (initial flat bed and low gate elevation) as well as the corresponding computed bed profiles. Also figure 6 presents the observed and computed bed profiles for run F2 illustrating the erosion of a previously formed front (high bottom gate elevation). Figure 7 shows the observed and computed sediment discharge and cumulative flushed sediment for run F0.

For both cases, the computed values agreed well with the observed ones, so this model can be used for prediction of bed changes in reservoirs with elongated plan-shape, provided that bed-load predominates in the formation of the deposits.

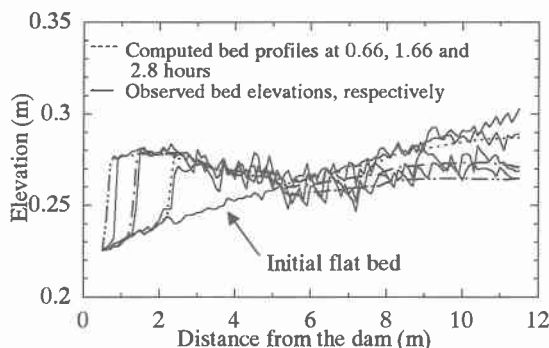


Figure 3: Experimental and calculated results for run D2

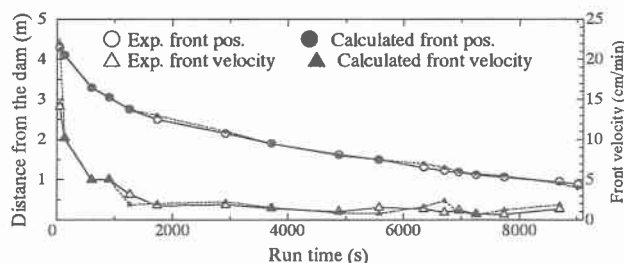


Figure 4: Observed and calculated position and velocity of the front for run D2

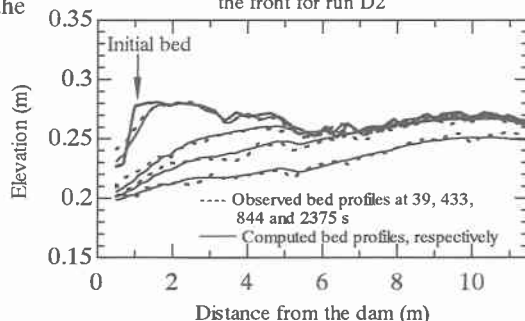


Figure 6: Experimental and calculated results for run F2

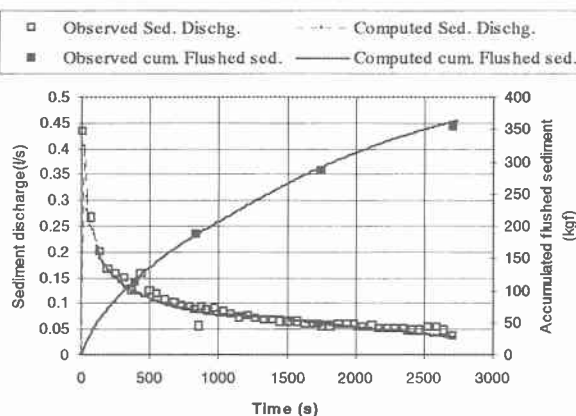


Figure 7: Experimental and calculated results for run F0